Available online at www.sciencedirect.com
SCIENCE DIRECT®
Planetary and Space Science 52 (2004) 1391–1398
Planetary and Space Science
www.elsevier.com/locate/pss

# Solar radar astronomy with the low-frequency array

Paul Rodriguez*

*Naval Research Laboratory, Information Technology Division, Transmission Technology Branch, 4555 Overlook Avenue, SW, Washington, DC 20375, USA*

Accepted 3 September 2004

**Abstract**

Initial studies of the Sun's corona using a solar radar were done in the 1960s and provided measurements of the Sun's radar cross-section at about 38 MHz. These initial measurements were done at a time when the large-scale phenomenon known as a coronal mass ejection was unknown; however, these data suggest that coronal mass ejections (CMEs) may have been detected but were unrecognized. That solar radar facility, which was located at El Campo, TX, no longer exists. New solar radar investigations are motivated by our modern understanding of CMEs and their effects on the Earth. A radar echo from an Earthward-directed coronal mass ejection may be expected to have a frequency shift proportional to velocity; thus providing a good estimate of arrival time at Earth and the possible occurrence of geomagnetic storms. Solar radar measurements may also provide new information on electron densities in the corona. The frequencies of interest for solar radars fall in the range of about 10–100 MHz, corresponding to the lower range planned for the low-frequency array. In combination with existing or new high-power transmitters, it is possible to use the low-frequency array to re-initiate radar studies of the Sun's corona. In this report, we review the basic requirements of solar radars, as developed in past studies and as proposed for future investigations.


*Keywords:* Solar radar; Coronal mass ejection; Radar cross-section

## 1. Introduction

In considering that the low-frequency array (LOFAR) will open a new window for radio astronomy (Kassim et al., 1998), it is also true that LOFAR, combined with high-power transmitters, will open a new window for low-frequency radar studies of our solar system. With the radar technique, many space plasma processes and interactions become accessible for study, and it is expected that entirely new scientific information on these phenomena will be acquired. We expect that among the most enticing research objectives of solar radars will be coronal mass ejections (CMEs), a large-scale dynamical process that is not well understood and for which low-frequency radar observations will provide a new research tool. The fact that CMEs are responsible for the largest geomagnetic storms on the Earth provides a practical motivating interest: the frequency shift imposed on the radar echo from a coronal mass ejection will measure the velocity component directed toward the Earth, thereby providing a good (perhaps the best) estimate of the CME's time of arrival at the Earth's orbit. Thus, an accurate forecast of a potential geomagnetic storm and its space weather effects is possible.

## 2. Background

The first proposal for solar radar research was published by Kerr (1952); this report was followed by a detailed study by Bass and Braude (1957). These two theoretical papers identified the basic instrumental requirements and emphasized the unique contribution to solar physics to be derived from solar radar

*Tel.: +1 202 767 3329; fax: +1 202 767 3377.
*E-mail address:* paul.rodriguez@nrl.navy.mil (P. Rodriguez).

0032-0633/$ - see front matter © 2004 Elsevier Ltd. All rights reserved.
doi:10.1016/j.pss.2004.09.008

measurements. There followed the first attempts to conduct solar radar experiments by groups from Stanford University (Eshleman et al., 1960) and the Lincoln Laboratory of the Massachusetts Institute of Technology (MIT) (Abel et al., 1961, 1963). The MIT group designed a solar radar facility for operation at 38.25 MHz, in which the same antenna array was used both to transmit and to receive the radio waves (James, 1966). This pioneering solar radar facility began operations near the town of El Campo, TX, in 1961. The principal scientific results from El Campo solar radar observations can be found in the review by James (1968), several succeeding papers (James, 1970a, b), and references therein. From the echo strengths measured at El Campo, the solar radar cross-section $\sigma$ was calculated. Each value of $\sigma$ required integration of the echo signal for the full round trip travel time to the Sun and back, or about 16 min (960 s) to achieve signal-to-noise ratios of about 5 to 6 dB above ambient background. The typical radar cross-section for the Sun's corona was found to be $\sigma \sim 1$, relative to the projected geometric area of the visible solar disk. However, a significant number of cross-sections were greater than 1, implying enhanced backscattering of the radio signal. This is illustrated in Fig. 1 by the plot of about 1000 values of $\sigma$ measured by the El Campo facility (James, 1970c). In order to show more clearly the variations of the cross-sections, we plot only values below 50, which constitute about 95% of the data. Cross-sections greater than 50 tend to be scattered over a wide range, with the maximum value of about 800. The radar cross-sections also showed a positive correlation with sunspot number, and this result was taken as indicating that increasing solar activity increased the echo strength. Frequency shifts in the echo signals of about 4–15 kHz or more were detected routinely and were attributed to mass motions associated with the outward flow of the solar wind from the base of the corona. Although the phenomenon of CMEs was unknown at the time of the El Campo operations, various interpretations of the data came close to what might be conceived of as coronal mass ejections. In fact, a subset of the El Campo data were classified as "high corona echoes." In retrospect, it is likely that the high corona echoes corresponded to CMEs.

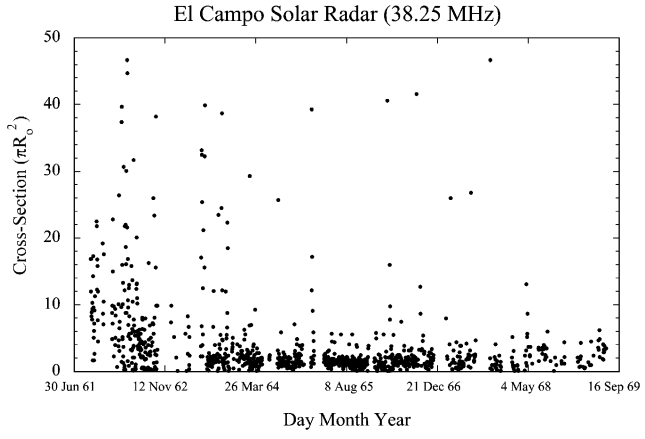


Fig. 1. The set of solar radar cross-sections measured by the El Campo solar radar array, during the years from 1961 to 1969.

The El Campo investigations have stimulated various theoretical studies and interpretations by Gordon (1968, 1969, 1973), Gerasimova (1975, 1979), Wentzel (1981), Owocki et al. (1982), Chashei and Shishov (1994), and Mel'nik (1999, 2003). These studies show that radar echoes can provide important new diagnostic information on the structure and dynamics of the solar corona. In the initial solar radar investigations and theoretical studies, the possibility of detecting CMEs was not specifically considered, because it was only in later years (the 1970s) after El Campo had ceased operations that CMEs were recognized as distinct large-scale coronal perturbations. Now that we know the link between CMEs and geomagnetic storms at Earth (reviewed in the monograph edited by Crooker et al., 1997), we can anticipate that solar radars will become a powerful technique to detect and diagnose Earthward-moving CMEs (Rodriguez, 1996). On the basis of the known distribution of CME velocities, we expect that velocity-induced frequency shifts, up to 100 kHz, would be imposed on the radar echo signal. The large-scale structures of CMEs may also result in radar cross-sections larger than those of the normal corona. Thus, the combination of frequency shifts and large cross-sections may be a distinct radar signature of CMEs.

More recently, the Sura ionospheric heating transmitters in Russia and the UTR-2 radio astronomy array in Ukraine were used in bistatic configuration to conduct low-frequency solar radar experiments (Rodriguez, 2000; Thide, 2002). Ionospheric heating is done with frequencies near the ionospheric plasma frequency, typically between 6 and 10 MHz, depending on the time of day and solar activity. By closely matching the transmitted frequency to the ionospheric plasma frequency, maximum absorption of the radio wave energy occurs with subsequent heating of ionospheric electrons. Of course, such absorption is not desired for solar radar studies, where we want as much energy as possible to propagate to the Sun. In order for the radio wave to be transmitted past the Earth's ionosphere, the radio wave frequency must exceed the ionospheric plasma frequency. This condition was met at Sura by transmitting at 9 MHz during times near local noon (the Sun overhead) and when the maximum ionospheric plasma frequency was about 6 MHz (solar activity at a minimum). Each experiment was of a 30-min duration and followed a operational sequence similar to that of the El Campo measurements; several of the experiments resulted in the detection of a weak solar echo. The

coronagraph images that were available indicated that no CMEs occurred during the times of these tests.

## 3. The solar radar window

The basis of solar radar measurements is that coronal electron densities are typically in the range corresponding to electron plasma frequencies from about 5 to 200 MHz. Various models have been developed for the radial dependence of electron densities in the quiescent corona; generally, these models are inverse power laws. In Fig. 2, we show several models (James, 1968; Allen, 1973; Saito et al., 1977; Coles and Harmon, 1989) for coronal electron density versus radial distances in the range from 1 to 40 $R_o$ (where $R_o$ is in solar radii). These radial dependencies may be converted into plasma frequency radial variations using the formula

$$f_{pe} = \sqrt{(N_e q_e^2)/(\pi m_e)}, \quad (1)$$

where the parameters are defined as $f_{pe}$ is the electron plasma frequency (Hz), $N_e$ the electron density ($cm^{-3}$), $q_e$ the electron charge (statcoulomb) and $m_e$ the electron mass (g).

The resulting curves for electron plasma frequency (in MHz) are shown in Fig. 3. Because coronal electron densities are mostly greater than electron densities in the Earth's ionosphere, the frequencies for a solar radar can be chosen to enable propagation through the Earth's ionosphere both on transmission and on return. The window of solar radar frequencies is in the range of about 10–100 MHz, determined on the low end by the Earth's ionospheric cutoff and on the high end by collisional absorption in the corona. A radio wave

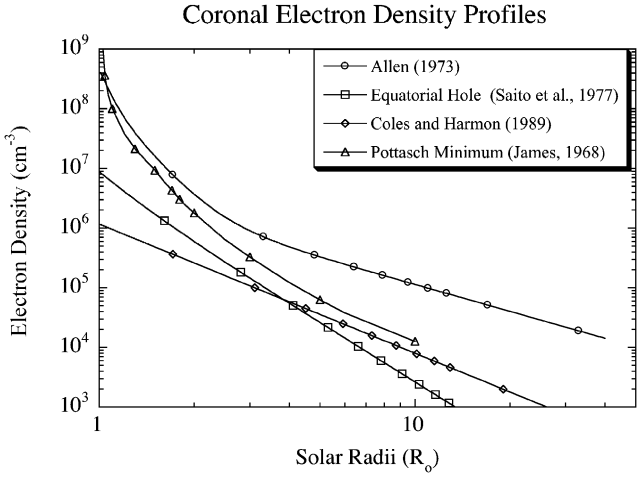


Fig. 2. Models of electron density in the corona, for radial distances in the range 1–40 solar radii ($R_o$).

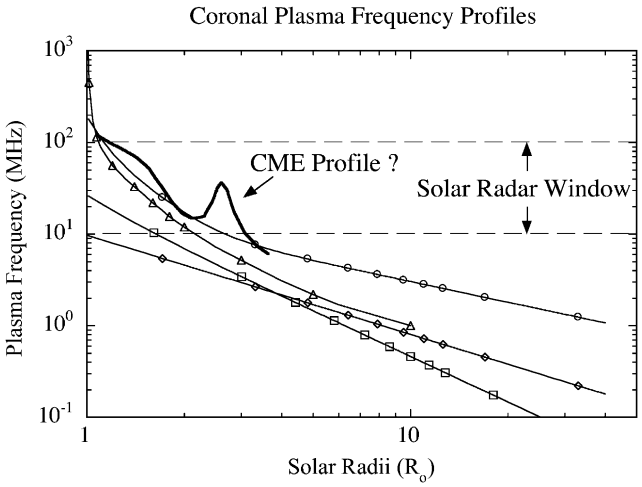


Fig. 3. Electron plasma frequency profiles in the corona, derived from the electron density models of Fig. 2. The solar radar window is in the range from about 10–100 MHz. A possible three-part CME profile in plasma frequency (proportional to electron density) is suggested.

transmitted from Earth propagates into the corona until the wave frequency equals the coronal plasma frequency, at which point the index of refraction rapidly decreases from the free-space value of 1 to a value of 0, resulting in backscattering of the radio wave. Although it serves as a working model, this wave scattering description is probably too simple. In a turbulent and structured corona, the echo signal may actually be the result of more complex wave–plasma interactions, which, if properly diagnosed, may provide information on coronal plasma structure. Coronagraph observations suggest that a CME may have a three-part structure, consisting of a leading edge, a following void or cavity, and a subsequent prominence core (Gosling, 1997). Flux rope models of CMEs (Gibson and Low, 1998; Chen et al., 2000; Chen and Krall, 2003; Krall and Chen, 2004) suggest that electron densities associated with the leading edge may be enhanced over the ambient density by factors of 7 or more. Low-frequency radio observations of the depletion behind a CME imply a very low electron density (Ramesh and Sastry, 2000). Thus, a three-part electron density profile of a CME would lead to a similar profile for electron plasma frequency (from $f_{pe} \sim \sqrt{N_e}$). If such a three-part profile occurs, as suggested in Fig. 3, then multiple frequency solar radar observations may provide a method to measure it, a technique that would be analogous to how ionospheric sounders measure the Earth's ionospheric density profile (Davies, 1990). Also, the presence of the coronal magnetic field means that the radio waves propagate in two characteristic modes, the so-called ordinary and extraordinary modes. This property also may be useful for solar radar studies of the corona (Cohen, 1960) and CMEs.

## 4. The radar equation

Solar radar measurements are governed by the radar equation

$$P_r = \frac{P_t G_t}{4\pi R^2} \frac{A_r \sigma p}{4\pi R^2}, \tag{2}$$

where the following parameters are defined as $P_r$ is the received echo power (W), $\sigma$ the radar cross-section (normalized by the projected area $\pi R_o^2$ of the solar disk), $P_t$ the transmitted power (W), $G_t$ the transmitting antenna gain, $p$ the polarization fraction, $A_r$ the receiving antenna area ($m^2$) and $R$ the range (m).

Numerical values are:

$R_o = 7 \times 10^8$ m (solar radius),

$\pi R_o^2 = 1.54 \times 10^{18}\,m^2$,

$R = 1.5 \times 10^{11}$ m (1 AU),

$p = 0.5$ (one of two polarizations).

The radar equation can be thought of as being composed of two factors. The first factor gives the power density incident on a target at distance $R$, where $P_t G_t$ is the effective radiated power (ERP) of the transmitted radio waves and $4\pi R^2$ is the surface area of a sphere centered on the transmitter. The second factor determines the power echoed by a target with effective cross-section $\sigma$ and, by dividing again by $4\pi R^2$, gives the echo power density incident on the receiving antenna. The echo power $P_r$ is then calculated by multiplying by the effective area $A_r$ of the receiving antenna and the antenna polarization fraction $p$. Because of the $R^{-4}$ dependence in the radar equation, we know that the echo power will be a small fraction of the transmitted power. Thus, we desire large values of $P_t G_t$ and $A_r$ to enable better detection of the echo. In the radar equation, all the physics of the radio wave interaction with the target is incorporated in $\sigma$; our research task is then to understand the processes determining this value.

The echo signal is always detected against a noise background, which includes noise from the receiving array system, the local environment, the galaxy, and radio emissions from the Sun itself. For solar quiescent conditions, the largest noise source will be the thermal emission of the Sun. We use this value as a minimum background noise level for estimating the signal-to-noise ratio of solar radar operations. The noise power associated with the solar thermal background is given by the equation

$$N = k_B T(f) B \tag{3}$$

where $k_B = 1.38 \times 10^{-23}\,W\,s\,K^{-1}$ (Boltzman's constant), $T(f)$ is noise equivalent temperature of the Sun (K) for given frequency $f$ and $B$ is receiver bandwidth (Hz).

Because of the expected low power of the echo, it is important to consider signal integration techniques to obtain higher values of the signal-to-noise ratio, $P_r/N$. The gain $G$ obtained by signal processing is derived by using the standard formula for integration with a random noise background

$$G \sim \sqrt{Bt}, \tag{4}$$

where $B$ is the receiver bandwidth and $t$ is the integration time.

## 5. LOFAR solar radar

Solar radar investigations combining operation of LOFAR with a high-power radio wave transmitter will form a *bistatic* radar configuration. In such a configuration, the LOFAR receiving antennas and the high-power transmitter are not co-located and may be separated by large distances. The only location requirement is that both facilities are able to view the Sun during the travel time of the radio waves to the Sun and back. The basic operational cycle of a solar radar is to transmit radio waves to the Sun for 16 min (the round trip light time for 1 AU) followed by 16 min of echo reception, or about 32 min of combined operation. To reduce possible interference, the transmitter is usually turned off during the 16 min of echo reception. However, if such interference can be minimized, then transmission and reception could be overlapped and the number of operational cycles increased. We desire as many of these basic operational cycles as possible, so that tracking of the Sun across the sky by both transmit and receive beams is required. With computer-controlled electronic phasing, it is possible to form and quickly point a beam in specified directions and to use null steering to reduce extraneous noise. Computer control also provides agility in changing the radio wave frequency and transmitter modulations. Thus, new solar radar studies should be able to track the Sun across the sky for several hours, and multiple investigations may be conducted daily. In addition, increased speed and volume of data acquisition and analysis, combined with advanced digital signal processing algorithms, will provide improved measurements. These modern technological capabilities will be significant for new solar radars. In comparison, the El qCampo solar radar was constrained to be a mechanically phased array that could operate in transit mode only, allowing only one measurement of cross-section per day, with the data obtained almost entirely in the analog regime.

Depending on the final location of LOFAR, several existing high power radio transmitting arrays are candidates to form the bistatic configuration. Among such facilities in the western hemisphere are the

HF Active Auroral Research Program (HAARP) transmitting array, the Arecibo radar facility, and the Jicamarca ionospheric array. In the eastern hemisphere, possible transmitters include the European Incoherent Scatter (EISCAT) transmitter, the Sura ionospheric heating transmitter, and several proposed new facilities. Even with high-power transmitters the radar echo from the Sun's corona will be weak, because of the great distance of propagation involved; thus, it is advantageous that LOFAR will have an effective receiving area of about 1 $km^2$ at low radio frequencies. The antenna gain of LOFAR and its planned imaging capabilities will allow for detailed analysis of the radar echo. Estimates of the signal-to-noise ratio for solar radar echoes as a function of the integration time required to achieve a specified detection level (e.g., ~5 dB above solar quiescent background) indicate that time resolutions of tens to hundreds of seconds can be achieved. Thus, we may be able to resolve solar radar echo variations on time scales that may be important in the dynamics of coronal mass ejections. For example, coronagraph images typically show displacement of CMEs over several solar radii on hourly time scales (Howard et al., 1997).

To develop a specific example of the solar radar capability, we use the basic system design of LOFAR in conjunction with the system characteristics of the HAARP transmitting array. Although HAARP is designed as an ionospheric heating transmitter, it is now also engaged in space radar experiments with operations similar to those required of a solar radar transmitter. HAARP is also an electronically phased array, with capability for fast beam tracking, modulation, and frequency agility. The location of HAARP at high latitudes (62.4°N, 145.1°W) makes it a potential bistatic partner only if LOFAR is located in the western United States, one of the three LOFAR candidate sites. The HAARP facility power is presently about 1 MW and will be increased in a few years to a total power of about 3.6 MW with an antenna gain of about 30 dB or more at 10 MHz, making it the most powerful transmitting array at low frequencies available for scientific research. In comparison, the total power at El Campo was about 500 kW with an antenna gain of about 32 dB at 38 MHz. The power transmitted at HAARP varies with zenith angle $\phi$ approximately as $\cos^2(\phi)$, and the beam can be pointed to $\phi \leqslant 50°$; about one-half the total power is available at $\phi = 45°$. The HAARP array will be capable of illuminating the Sun for daily intervals of about 2–3 h about noontime, for about 3 months centered on summer solstice, when the Sun has zenith angles of about $40° \geqslant \phi \geqslant 50°$. For these periods, the Sun's zenith angle at LOFAR (if located in the western United States) would be about $15° \geqslant \phi \geqslant 45°$. Under these conditions, the effective radiated power to the Sun from HAARP will be about three times larger than the El Campo solar radar provided. If LOFAR is located at one of the other two candidate sites, The Netherlands or western Australia, HAARP cannot view the Sun simultaneously with LOFAR, and different transmitters would have to be considered. All existing transmitting facilities have limitations of one kind or another as potential bistatic partners with LOFAR because none have been designed specifically as solar radars and because none are near the candidate sites (one criterion for the LOFAR site is that there be low noise background from ambient transmitters). Obviously, a new transmitting facility specifically designed for LOFAR solar radar operations at its selected site would provide the ideal configuration. Such a facility would have system characteristics similar to those of HAARP, with the additional feature of allowing higher frequencies of transmission, in order to cover the entire solar radar window. Therefore, in our example of solar radar performance, we use the parameters of HAARP as representative of the basic transmitter characteristics desired. We summarize the system parameters of HAARP and LOFAR in Table 1, where we now refer to the bistatic configuration as the "HALO" configuration.

The variation of power density transmitted from HAARP over a range of 1 AU is shown in Fig. 4 for the current power level and the design power level of HAARP. This plot shows the variation of the first factor of the radar equation for these two power levels. The range is in units of solar radii ($R_o$), with the distances of the Moon and Sun indicated. We also show the average galactic background noise density at about 10 MHz (Tokarev, 2001). In addition, the noise threshold of the WAVES radio receiver on board the NASA/WIND spacecraft is shown for comparison (Bougeret et al., 1995). HAARP has conducted many experiments with the WAVES radio receiver (Rodriguez et al., 1998) to distances of about four times the Moon's distance, and it is a convenient performance measure to use. From Fig. 4 we may derive several insights. At current power level, the HAARP radiated power density is above both galactic background and WAVES threshold at distances out to about 100 $R_o$ (~ the orbit of Venus), so it would be possible to detect HAARP at this distance with the WAVES receiver. With sufficient signal integration, WAVES would also be able to detect HAARP at 1 AU against the galactic background. At the design power level of HAARP, the plot shows that WAVES should be able to detect HAARP at 1 AU directly, with minimal signal integration. The WAVES receiver utilizes only a single dipole antenna and thus has a relatively small effective receiving area compared with a large Earth-based array like LOFAR. However, for solar radar studies, because the echo signal must propagate another distance of 1 AU on the return path to Earth and would thus continue to decrease in power density, the larger

Table 1
HALO system parameters

| | Current facility | Design facility |
|---|---|---|
| *HAARP* | | |
| Radiated power | 960 kW | 3600 kW |
| Frequency coverage | 2.8–8.2 MHz | 2.8–10 MHz |
| Antenna gain | 13–23 dB | 20–31 dB |
| Effective radiated power | 20–200 MW | 400–3000 MW |
| Antenna beamwidth | 9–32° | 4.5–15° |
| Zenith angle ($\phi$) pointing* | 0–30° | 0–30° |
| Location | Gakona, Alaska (62.4°N, 145.1°W) | |
| *LOFAR* | | |
| Fully electronic, broad-band antenna array | | |
| Active dipole antennas covering radio frequencies ~10–250 MHz | | |
| Multiple beams: new approach to astronomical observations | | |
| Large collecting area $\geqslant 10^6\,m^2$ (2–3 orders of magnitude improvement in resolution and sensitivity) | | |
| Antenna beamwidth ~8″ at 15 MHz | | |
| Candidate site locations: | Western United States (New Mexico) | |
| | The Netherlands | |
| | Western Australia | |

*Larger zenith angle is possible, with power variation $\sim\cos^2(\phi)$.

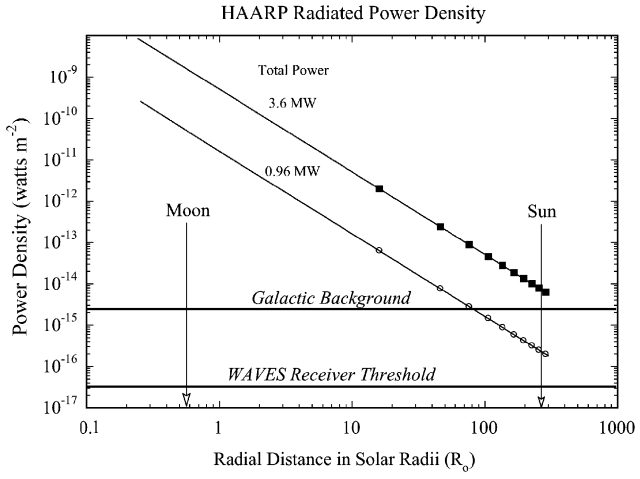


Fig. 4. Radiated power density from HAARP as a function of radial distance toward the Sun, for current and design power levels. Galactic background and WAVES receiver noise thresholds are shown for comparison.

effective area of LOFAR becomes an important system parameter.

We may use the parameters listed in Table 1 in conjunction with the radar equation, the thermal noise background, and signal integration to determine the performance characteristics of the HALO system as a solar radar. In this bistatic calculation, the HAARP characteristics provide the first factor in the radar equation, as shown in Fig. 4. The second factor of the radar equation is determined by LOFAR characteristics, for specific values of the cross-section $\sigma$. The noise background is taken to be that of the quiescent Sun. We define the system performance as given by the net signal-to-noise ratio of the solar radar echo as a function of the integration time. For specific values, we take the frequency of transmission to be $f = 10$ MHz, the receiving area $A_r \sim 10^6\,m^2$, the receiver bandwidth $B = 50$ kHz, and the solar noise temperature $T(10\,\text{MHz}) \sim 3 \times 10^5$ K. For solar radar cross-section, we take the two values $\sigma = 1$ and $\sigma = 10$ as representative of the El Campo measurements shown in Fig. 1. We note that solar radar cross-sections for CMEs may vary with the radio wave frequency because of spatial variations of electron densities along the radial and transverse directions from the Sun. For our performance calculation, however, we assume that the cross-sections measured at 38 MHz by El Campo are representative of all frequencies. We also include a loss of signal strength of about 2 dB from two-way propagation through the Earth's ionosphere. Fig. 5 shows the resulting performance of HALO under the assumed conditions and where we have taken the detection threshold requirement to be 5 dB. The lowest curve in the plot is the signal-to-noise ratio for a solar radar cross-section of 1 and the current power level of HAARP and indicates that it would be necessary to integrate the echo signal for about 10 s in order to reach the 5 dB detection threshold. The higher level curves correspond to either larger transmitted power or larger cross-section. For all curves, integrating for longer periods of time increases the signal-to-noise ratio. The

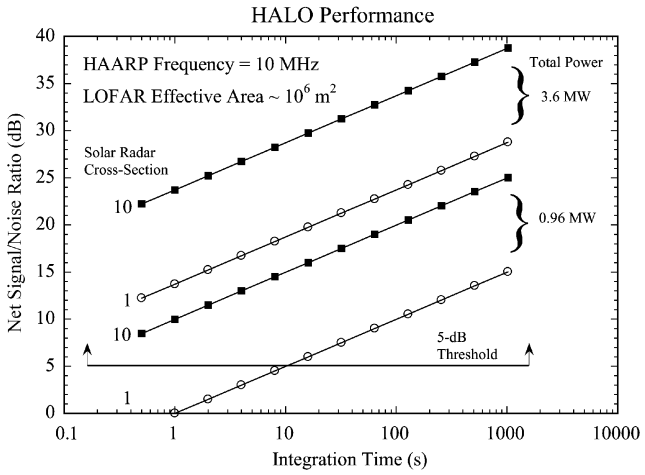


Fig. 5. The performance of the bistatic HAARP-LOFAR (HALO) configuration as a solar radar. Performance is measured as the net signal-to-noise ratio for the radar echo as a function of the integration time.

integration time is an important consideration for solar radar measurements because it also determines the time resolution of the measurement of the cross-section. Longer integration times increase the signal-to-noise ratio but also reduce the time resolution. As may be expected, with higher power levels or larger cross-sections, we can meet the detection threshold with shorter integration times. Depending on what additional noise sources are included, such as active solar radio emission, the family of curves would be shifted down, reducing the net signal-to-noise ratios possible and the integration time would have to be adjusted according to the signal-to-noise ratios experienced. If intense solar radio emission occurs, an echo signal may not be detectable above the threshold. We expect that differing echo strengths will result for different coronal conditions, e.g., the presence or absence of a CME. If we assume 100-s integration times are required for typical echo strengths during the daily 2- to 3-h intervals mentioned above, we obtain about 3000 to 4000 measurements of cross-section during the summer 3-month period. This would be 3 to 4 times as many measurements as acquired by El Campo in 8 yr of operation. Year-round operations with a transmitting facility specifically designed for LOFAR would increase proportionally the number of measurements possible. We may also relate HALO performance with the performance of the El Campo solar radar. Each daily cross-section measurement at El Campo required signal integration for about 16 min (960 s) to achieve signal-to-noise ratios of about 5–6 dB. In Fig. 5, we have thus set the 5-dB detection threshold and maximum integration time at 1000 s to represent the El Campo performance. Thus, the performance plots indicate that we may expect to get relatively good performance from HALO, or other similar bistatic configuration, as a solar radar.

## 6. Summary and conclusions

We have discussed and reviewed the highlights of solar radar measurements and the potential for using LOFAR as the receiving array of a modern solar radar observatory. The El Campo solar radar provided the vanguard facility in the study of the solar corona with the radar echo technique. Because no facility comparable to El Campo exists today, LOFAR in combination with several possible existing transmitters, or with a specially designed new transmitter, offers the best opportunity to re-establish this important area of research. A measure of solar radar performance expected in a bistatic configuration is obtained by considering the specific example of LOFAR as the receiving array and HAARP as the transmitting array. This calculation indicates that a significant improvement over the El Campo performance is possible, allowing much better studies of the corona. One of the important benefits of solar radar investigations will be found in the study of coronal mass ejections, which can supply crucial information for current understanding of CMEs and their effects on the Earth. Low-frequency radar observations of solar system plasmas like the Sun's corona will also expand the fields of research in radar astronomy. Thus, we conclude that solar system research with solar radars is poised for a promising new beginning.

## Acknowledgements

We thank the Office of Naval Research, the Naval Research Laboratory and the Air Force Office of Scientific Research for support of this research.

## References

Abel, W.G., Chisholm, J.H., Fleck, P.L., James, J.C., 1961. Radar reflections from the sun at very high frequencies. J. Geophys. Res. 66, 4303–4307.

Abel, W.G., Chisholm, J.H., James, J.C., 1963. Radar reflections from the sun at VHF. In: Priester, W. (Ed.), Space Res. III. North Holland Publishers, Amsterdam.

Allen, C.W., 1973. Astrophysical Quantities, third ed. The Athlone Press, University of London.

Bass, F.G., Braude, S.Ya., 1957. On the question of reflecting radar signals from the sun. Ukr. J. Phys. 2, 149–164.

Bougeret, J.-L., Kaiser, M.L., Kellogg, P.J., Manning, R., Goetz, K., Monson, S.J., Monge, N., Friel, L., Meetre, C.A., Perche, C., Sitruk, L., Hoang, S., 1995. WAVES: the radio and plasma wave investigation on the WIND spacecraft. Space Sci. Rev. 71, 231–263.

Chashei, I.V., Shishov, V.I., 1994. Volume scattering model for interpretation of solar radar experiments. Sol. Phys. 149, 413–416.

Chen, J., Santoro, R.A., Krall, J., Howard, R.A., Duffin, R., Moses, J.D., Brueckner, G.E., Darnell, J.A., Burkepile, J.T., 2000. Magnetic geometry and dynamics of the fast coronal mass ejection of 1997 September 9. Astrophys. J. 533, 481–500.

Chen, J., Krall, J., 2003. Acceleration of coronal mass ejections. J. Geophys. Res. 108 (11), 1410.

Cohen, M.H., 1960. High-frequency radar echoes from the Sun. Proc. IRE 48, 1479.

Coles, W.A., Harmon, J.K., 1989. Propagation observations of the solar wind near the sun. Astrophys. J. 337, 1023–1034.

Crooker, N., Joselyn, J.A., Feynman, J. (Eds.), 1997, Coronal Mass Ejections. Geophysical Monograph 99, American Geophysical Union.

Davies, K., 1990. Ionospheric Radio. Peter Peregrinus Ltd., London, UK.

Eshleman, V.R., Barthle, R.C., Gallagher, P.B., 1960. Radar echoes from the sun. Science 131, 329–332.

Gerasimova, N.N., 1975. Comparison of results of radar studies of the corona with solar activity. Sov. Astron. 18, 482–485.

Gerasimova, N.N., 1979. Efficiency of four-plasmon interactions in the reflection of a radar signal from the sun. Sov. Astron. 23, 738–740.

Gibson, S.E., Low, B.C., 1998. A time-dependent three-dimensional magnetohydrodynamic model of the coronal mass ejection. Astrophys. J. 493, 460–473.

Gordon, I.M., 1968. Interpretation of radio echoes from the sun. Astrophys. Lett. 2, 49–53.

Gordon, I.M., 1969. Radar exploration of the sun and physical processes of the solar corona. Astrophys. Lett. 3, 181–188.

Gordon, I.M., 1973. Plasma theory of radio echoes from the sun and its implications for the problem of the solar wind. Space Sci. Rev. 15, 157–204.

Gosling, J.T., 1997. Coronal mass ejections: an overview. In: Crooker, N., Joselyn, J.A., Feynman, J. (Eds.), Coronal Mass Ejections. Geophysical Monograph 99, American Geophysical Union.

Howard, R.A., Brueckner, G.E., St. Cyr, O.C., Biesecker, D.A., Dere, K.P., Koomen, M.J., Korendyke, C.M., Lamy, P.L., Llebaria, A., Bout, M.V., Michels, D.J., Moses, J.D., Paswaters, S.E., Plunkett, S.P., Schwenn, R., Simnett, G.M., Socker, D.G., Tappin, S.J., Wang, D., 1997. Observations of CMEs from SOHO/LASCO. In: Crooker, N., Joselyn, J.A., Feynman, J. (Eds.), Coronal Mass Ejections. Geophysical Monograph 99, American Geophysical Union.

James, J.C., 1966. Radar studies of the sun at 38 Mc/s. Astrophys. J. 146, 356–366.

James, J.C., 1968. Radar studies of the sun. In: Evans, J.V., Hagfors, T. (Eds.), Radar Astronomy. McGraw-Hill Book Company, New York.

James, J.C., 1970a. Some observed characteristics of solar radar echoes and their implications. Sol. Phys. 12, 143–162.

James, J.C., 1970b. Some characteristics of the solar atmosphere that may be investigated by a VHF antenna system. Technical Report 32-1475. Jet Propulsion Laboratory, Pasadena, California.

James, J.C., 1970c. El Campo solar radar data and system design notes. Massachusetts Institute of Technology. Center for Space Research Technical Report-70-2. Boston, Massachusetts.

Kassim, N.E., Lazio, T.J., Erickson, W.C., 1998. Opening a new window on the universe: high resolution, long wavelength radio astronomy. Report to the Radio and Submillimeter Astronomy Panel of the National Academy of Sciences' Decadal Survey Committee.

Kerr, F.J., 1952. On the possibility of obtaining radar echoes from the sun and planets. Proc. IRE 40, 660–666.

Krall, J., Chen, J., 2004. A flux-rope model of CME rim-cavity density structure. Paper in preparation.

Mel'nik, V.N., 1999. Radar scattering by anisotropic Langmuir turbulence. Sol. Phys. 184, 363–367.

Mel'nik, V.N., 2003. Plasma theory of solar radar echoes. Radio Sci. 38 (3), 1036.

Owocki, S.P., Newkirk, G.A., Sime, D.G., 1982. Radar studies of the non-spherically symmetric solar corona. Sol. Phys. 78, 317–331.

Ramesh, R., Sastry, Ch.V., 2000. Radio observations of a coronal mass ejection induced depletion in the outer solar corona. Astron. Astrophys. 358, 749–752.

Rodriguez, P., 1996. High frequency radar detection of coronal mass ejections. In: Balasubramaniam, K.S., Keil, S.L., Smartt, R.N. (Eds.), Solar Drivers of Interplanetary and Terrestrial Disturbances. ASP Conference Series 95, pp. 180–188.

Rodriguez, P., 2000. Radar studies of the solar corona: a review of experiments using HF wavelengths. In: Stone, R.G., Weiler, K.W., Goldstein, M.L., Bougeret, J.-L. (Eds.), Radio Astronomy at Long Wavelengths. Geophysical Monograph 119, American Geophysical Union.

Rodriguez, P., Kennedy, E.J., Keskinen, M.J., Siefring, C.L., Basu, Sa., McCarrick, M., Preston, J., Engebretson, M., Kaiser, M.L., Desch, M.D., Goetz, K., Bougeret, J.-L., Manning, R., 1998. The WIND-HAARP experiment: initial results of high power radio-wave interactions with space plasmas. Geophys. Res. Lett. 25 (3), 257–260.

Saito, K., Poland, A.I., Munro, R.H., 1977. A study of the background corona near solar minimum. Sol. Phys. 55, 121–134.

Thide, B., 2002. Radio Studies of Solar-Terrestrial Relationships. Report by the LOIS science team.

Tokarev, Y.V., 2001. Cosmic background at long wavelengths. Radio Sci. 36, 1733–1737.

Wentzel, D.G., 1981. A new interpretation of James's solar radar echoes involving lower-hybrid waves. Astrophys. J. 248, 1132–1143.